Research Square

Preprints are preliminary reports that have not undergone peer review.
They should not be considered conclusive, used to inform clinical practice,
or referenced by the media as validated information.

CRISPRi loss-of-function mutations revealed through experimental evolution in Burkholderia cenocepacia

Zayra Batun
University of Manitoba
Erick E. Arroyo-Pérez
Université de Montréal and Institut Courtois d'Innovation Biomédicale
A. S.M. Zisanur Rahman
University of Manitoba
Marike Palmer
University of Manitoba
Andrew M. Hogan
University of Manitoba
Sion Yi
University of Manitoba
Yves V. Brun
Université de Montréal and Institut Courtois d'Innovation Biomédicale
Silvia T. Cardona
silvia.cardona@umanitoba.ca

University of Manitoba

Article

Keywords: Essential genes, CRISPR interference (CRISPRi), gene repression, reversion mutants, transcription regulation, dCas9

Posted Date: July 17th, 2026

DOI: https://doi.org/10.21203/rs.3.rs-9728301/v1

License: This work is licensed under a Creative Commons Attribution 4.0 International License.
Read Full License

Additional Declarations: No competing interests reported.

Abstract

Essential genes encode proteins required for cell growth and survival, which makes them ideal targets for controlling bacterial growth during infection or in industrial applications. A gene silencing approach, CRISPR interference (CRISPRi), enables transcriptional control of essential genes, allowing phenotypic characterization of knockdown mutants. We previously developed a CRISPRi system for the Gram-negative bacteria Burkholderia, consisting of a chromosomally encoded rhamnose-inducible dCas9 and a plasmid encoding constitutively expressed synthetic guide RNAs (sgRNAs) targeting essential genes. Despite the system's utility, the CRISPRi mutants often reverted to wild-type growth phenotypes, hindering their use in gene-to-function studies that require many generations. To understand the reasons for the CRISPRi mutants' phenotypic reversions, we performed experimental evolution of 15 CRISPRi mutants under dCas9-inducing and non-inducing conditions, followed by quantitative gene expression analysis and whole-genome sequencing (WGS). While the CRISPRi machinery remained genetically stable in the CRISPRi-evolved mutants, reverse transcription quantitative PCR revealed a loss of CRISPRi repression in several mutants. Immunoblotting analysis further demonstrated that dCas9 expression was abolished, suggesting a defect in rhamnose uptake. One evolved CRISPRi mutant showed single-nucleotide polymorphisms (SNPs) affecting putative ABC sugar transporters. This work highlights the strengths and limitations of CRISPRi-based downregulation of essential genes for extended control of bacterial growth.

Introduction

Essential genes encode products or cellular processes that are indispensable for bacterial growth and survival [1]. However, establishing direct gene-to-function relationships for these genes remains particularly challenging, as their genetic manipulation in bacteria is inherently constrained [2]. In contrast to non-essential genes, bacterial essential genes cannot be studied by classical deletion mutagenesis because their removal is lethal, precluding the construction of viable knockout strains. Consequently, genetic tools that enable tunable, reversible, or partial suppression of essential gene expression are required to systematically interrogate essential gene function while preserving cell viability.

CRISPR (clustered regularly interspaced short palindromic repeats) interference or CRISPRi has emerged as an effective genetic tool for essential gene functional studies [3]. The CRISPRi system consists of an inducible Cas9 with no exonuclease activity or dead Cas9 (dCas9) [4] and a target-specific synthetic guide RNA (sgRNA) designed toward the target gene and adjacent to a critical protospacer-adjacent motif (PAM). The sgRNA guides dCas9 binding to the target gene, causing inhibition of gene expression by steric impediment of RNA polymerase activity. The effect of silencing an essential gene can then be regulated by modulating the levels of the dCas9, which has been applied in several studies of essential genes [5, 6]. Although powerful, the strong selective pressure driven by the downregulation of essential genes can select spontaneous mutations in the CRISPRi machinery, which compromise its effectiveness during essential gene functional characterizations [7, 8].

We previously developed CRISPRi for the bacterial genus *Burkholderia.* Our CRISPRi toolkit (Fig. 1) consists of a chromosomally-located dCas9 from *Streptococcus pyogenes* under control of a rhamnose-inducible promoter [6] and a plasmid expressing gRNAs. This system demonstrated downregulation of essential gene expression at the genome level by targeting over 500 essential genes in *Burkholderia cenocepacia* K56-2 [9], an opportunistic pathogen in people living with cystic fibrosis [10–12].

In this study, we used experimental evolution to investigate the genetic stability of the CRISPRi system in *Burkholderia cenocepacia* K56-2 under conditions of essential gene repression. Across mutants, we observed reversion to wild-type–like growth at distinct time points, reflecting loss of rhamnose-dependent, conditional growth phenotypes (CGPs). Although the CRISPRi machinery remained intact, dCas9 expression was lost in all evolved mutants. Whole-genome sequencing revealed that one evolved mutant showed deletions and insertions in putative ABC sugar transporters, suggesting that lack of rhamnose uptake could cause the CRISPRi system to turn off. Together, our results highlight Burkholderia's genetic adaptability to overcome CRISPRi-mediated gene silencing, suggesting ways to enhance the stability of essential gene conditional phenotypes.

Results

Conditional Growth Phenotypes are COG-independent and Diverse Across CRISPRi Essential Gene Mutants

To characterize CRISPRi conditional growth phenotypes (CGPs) spanning different general functions of essential genes, we selected fifteen CRISPRi mutants (**Supplementary Table 1**) spanning different Cluster of Orthologous Genes (COG) functional categories: cell division (COG D), cell envelope biogenesis (COG M), DNA replication and repair (COG L), energy production (COG C), translation (COG J) and nucleotide conversion and metabolism (COG F) **(Supplementary Table 2).**

We monitored bacterial growth for 24 h under dCas9-inducing (0.5% rhamnose) and non-inducing (0% rhamnose) conditions (Fig. 2). CRISPRi mutants targeting essential genes within the same COG category displayed distinct CGPs, revealing functional heterogeneity despite shared functional classification. Based on prolonged lag phases relative to non-induced controls, mutants were stratified along a continuum of growth defects, ranging from severe to mild. Notably, under sustained dCas9-inducing conditions, all CRISPRi mutants ultimately achieved a final optical density comparable to non-induced controls, consistent with a progressive loss of CRISPRi-mediated repression of essential gene expression.

Short-term Evolution Experiment Reveals CGP Loss at Different Bacterial Passages

To interrogate the genetic stability of CRISPRi-mediated repression of essential genes and its susceptibility to adaptive escape, we subjected CRISPRi mutants to a short-term experimental evolution assay (Fig. 3). Mutants were serially passaged for three consecutive rounds under dCas9-inducing conditions, thereby imposing continuous selective pressure for the attenuation or loss of CRISPRi-dependent growth inhibition. All fifteen CRISPRi mutants exhibited CGP loss at distinct time points, occurring after one, two, or three passages. In contrast, CGPs were stably maintained when overnight cultures were propagated under non-inducing conditions (**Supplementary Figs. 1–15**), indicating that repression escape was specifically associated with dCas9 induction. As expected, the non-targeting sgRNA control (NTC) strain retained a wild-type–like phenotype throughout all passages (**Supplementary Fig. 16**). Notably, the number of necessary passages for observing a CGP loss was not related to any particular COG functional category, suggesting that CRISPRi escape is governed by target- or CRISPRi system-specific determinants rather than broad functional classes of essential genes.

K-medoids Reveals Three Clusters Based on Growth Curve Parameters

To quantitatively compare growth dynamics among the CRISPRi mutants, we extracted growth parameters (**Supplementary Table 3**) from growth curves of all passages and fitted the data to a logistic model using Growthcurver [13] (see Material and Methods for details). The analysis revealed 3 distinct clusters with five CRISPRi mutants in Cluster 1, two CRISPRi mutants in Cluster 2, and eight CRISPRi mutants in Cluster 3 (Fig. 4A); the latter of which included the NTC control mutant. Cluster 1 mutants exhibited pronounced growth defects characterized by extended apparent lag phases, reduced terminal optical density, and rapid CGP loss after a single passage under sustained dCas9-inducing conditions. Cluster 2, in which parental strains displayed a moderate growth defect under consistent dCas9-inducing conditions, was characterized by a prolonged apparent lag time after the first passage and CGP loss after subsequent passages. In contrast, Cluster 3 mutants exhibited only mild growth defects and variable timing of CGP loss under consistent dCas9-inducing conditions. (Fig. 4B **and Supplementary Fig. 17**).

Conditional Growth Phenotype Reversion analyzed by RT-qPCR Detection of CRISPRi target genes and dCas9 expression analysis

Based on prior reports identifying CGP escape- associated mutations in sgRNA and dCas9 coding sequences [7, 8], we tested whether the observed loss of the CGP resulted from alleviation of our CRISPRi- based essential gene silencing system or produced by suppressor mutations. To this end, we used RT- qPCR to quantify essential gene expression in 11 CRISPRi knockdown mutants, including 5 from Cluster 1 (Fig. 5), 2 from Cluster 2, and 4 representative mutants from Cluster 3 (**Supplementary Fig. 18**). Parental strains from Cluster 1 exhibited 5- to 79- fold reductions in target gene expression under dCas9-inducing conditions relative to non- inducing controls. This repression was lost in the evolved CRISPRi mutants *dcw*, *dnaN*, *gyrB*, and *gatB* after passage 1 under continued dCas9 induction

(Fig. 5A). In contrast, the CRISPRi *atpB* mutant showed persistent gene silencing after passage 1. In Cluster 2, the CRISPRi *ligA* mutant displayed a strong 46- fold reduction in target gene expression in the parental strain, whereas the *engA* mutant showed a more modest 7. 4- fold reduction **(Supplementary Fig. 18**). Notably, transcript levels for both mutants increased following one and two overnight passages under sustained dCas9- inducing conditions, ultimately exceeding those observed under non- inducing control conditions. Lastly, Cluster 3 exhibited the greatest variability in gene expression across passages (**Supplementary Fig. 18**). The CRISPRi *trxB* mutant exhibited a 52- fold reduction in gene expression in the parental strain; however, relative expression levels progressively increased under consistent dCas9-inducing conditions, ultimately exceeding those in non- inducing controls. In contrast, the CRISPRi *parAB* mutant showed no repression in the parental strain and fluctuating gene expression across passages under dCas9- inducing conditions (**Supplementary Fig. 18**).

To further investigate the relationship between phenotypic outcomes and CRISPRi-targeted gene expression levels, we prioritized Cluster 1 for deeper analysis. Because de-repression of CRISPRi silencing in the *dcw*, *dnaN*, *gyrB*, and *gatB* mutants suggested loss of dCas9 expression, we performed immunoblot analysis of parental and evolved strains using anti-Cas9 antibodies. As expected, dCas9 was detected in all parental CRISPRi mutants as well as in the parental and evolved NTC controls. In contrast, no detectable dCas9 signal was observed in the evolved *dcw, dnaN, gyrB*, and *gatB* mutants (Fig. 5B, **Supplementary Fig. 19–20**), consistent with the de-repression of target gene expression detected in these evolved strains (Fig. 5A). Similarly, dCas9 was not detected in the evolved *atpB* mutant, despite continuous repression of the target gene. Together these findings demonstrate restoration of essential gene expression in the evolved mutants is linked to loss of dCas9 expression. The evolved *atpB* mutant represented an exception, maintaining repression of the target gene despite the absence of detectable dCas9.

Whole Genome Sequencing (WGS) Uncover Spontaneous Mutations related to CGP loss

To test whether spontaneous genetic changes underpinned the rapid alleviation of the CGP, we performed whole-genome sequencing on both parental non-induced strains and dCas9-induced evolved strains after a single passage. This analysis included all CRISPRi mutants from Cluster 1, as well as the NTC control strain, comprising whole-genome sequencing of 12 strains. Genomic DNA was sequenced using Oxford Nanopore Technology (ONT), with a minimum coverage depth of 150× for each genome. De novo assemblies were generated using Flye and consistently resolved into five contigs corresponding to the three chromosomes, one mega plasmid, and the sgRNA/trimethoprim resistance plasmid (pgRNA). To enable comparative genomic analyses, assemblies were manually reordered to standardize contig orientation and starting positions. Pairwise genome alignments were then performed using Minimap2, and single-nucleotide polymorphisms (SNPs) were identified using SyRI.

No mutations in the CRISPRi machine (dCas9 gene, rhamnose-inducible system, or sgRNA-encoded DNA sequences were identified. However, pairwise comparisons between each parental and evolved strains identified single-nucleotide polymorphisms (SNPs), which were subsequently mapped to affected genes (**Supplementary Table 5**). Several parallel mutant alleles found in the CRISPRi evolved mutants were also found in the CRISPRi evolved NTC control, likely representing random mutations unrelated to the selective pressure imposed by silencing an essential gene (**Supplementary Table 6**). In addition, some mutations found in the evolved strains were similar to the wild type reference genome likely representing random reversions to reference alleles and were filtered out for further analysis (**Supplementary Table 6**). A summary of the unique mutations that resulted from this analysis is shown in **Supplementary Table 7**. No suppressor mutations were found in the *atp* evolved mutant that could explain the loss of the CGP despite target gene silencing. Four evolved CRISPRi mutants *dcw*, *dnaA*, *gatB* and *gyrB* accumulated unique mutations. Among them, the *gyrB* mutant presented deletions and insertions interrupting sugar ABC transport system genes.

Discussion

Essential genes have been studied for decades, yet defining a universal core set that explains the foundations of cellular life remains challenging [2]. Genetic tools such as CRISPR interference (CRISPRi) enable tunable and conditional repression of essential genes, thereby facilitating functional interrogation of processes required for bacterial growth and survival. Beyond basic discovery, these approaches support a broad range of applications, including systematic identification of antibacterial drug targets, programmable control of microbial growth, and the development of genetic containLiument strategies for environmental and biotechnological applications. [14–16]. Despite these advantages, the long-term stability of engineered genetic systems remains insufficiently characterized. CRISPRi mutant populations may be highly susceptible to the selection of spontaneous escape mutations due to the strong selective pressure imposed by repression of essential genes. Indeed, studies using inducible CRISPRi systems in *Bacillus subtilis* and *Streptococcus pneumoniae* have shown that repeated subculturing under inducing conditions leads to rapid loss of conditional growth phenotypes (CGPs), driven by frameshift mutations within the *dCas9* coding sequence [7, 8] .

Here, we selected essential gene mutants from a CRISPRi library built in *Burkholderia cenocepacia* K56-2 to evaluate the stability of CRISPRi-mediated repression of essential genes and determine whether spontaneous adaptive events could undermine its function. Across all mutants tested, the conditional growth phenotype (CGP) was lost, with individual mutants exhibiting CGP collapse after one, two, or three passages and ultimately recovering wild-type–like growth. Unsupervised K-medoids clustering further resolved the mutants into three distinct groups, primarily differentiated by the duration of their apparent lag phase. To determine whether the clustering patterns reflected differences in repression efficiency, we quantified target gene expression by RT-qPCR in all mutants from Clusters 1 and 2 and in four representative mutants from Cluster 3. and integrated these data with phenotypic and clustering outcomes across passages. There was a strong concordance between target gene expression recovery and CGP loss in Cluster 1 with exception of the *atpB* mutant in which the was lost but no significant

alleviation of the target gene silencing effect was observed. In all evolved mutants examined, expression of dCas9 was not detected (Fig. 5B). However, no mutations were detected within components of the CRISPRi machinery itself that could explain the absence of dCas9, suggesting that the evolved mutants accumulated defects in rhamnose transport across the cell envelope, which in turn could cause lack of dCas9 expression.

In the CRISPRi system developed for *Burkholderia*, the *dCas9* gene is under the rhamnose-inducible *Escherichia coli* P_{rhaB} promoter [17]. A rhamnose transporter *rhaT*, is encoded in the original L-rhamnose utilization gene cluster [18]. However, the CRISPRi system developed in Burkholderia does not include *rhaT* [19, 20], implying that endogenous Burkholderia transport systems can internalize rhamnose. Notably, no *rhaT* homologs have been identified in *Burkholderia* genomes, and the genetic basis of rhamnose uptake in this genus remains unresolved. As the *gyrB* mutant accumulated mutations in ABC sugar transporters it is likely that these systems may have in rhamnose uptake. While this is a likely explanation for the evolved *gyrB* mutant phenotype, the other evolved CRISPRi mutants did not present unique mutations in sugar transport genes, yet dCas9 expression was not detected despite an intact CRISPRi system.

A likely explanation is that growth under the strong selective pressure of silencing essential genes selected evolved CRISPRi mutants that lost rhamnose transporters by a epigenetic mechanism [21]. Indeed, the “all-or-nothing” induction is well known in bacterial sugar utilization systems. This condition arises from positive feedback between sugar transport and gene induction. The inducer sugar must first enter the cell through specific transporters distributed in the cell envelope randomly. While expression of those same transporters is activated by the intracellular inducer, differences in transporter abundance between individual cells can produce dramatically different outcomes: cells with enough transporters accumulate sufficient inducer to activate the regulatory circuit, leading to even greater transporter expression and a fully induced ON state, whereas cells with fewer transporters fail to reach the activation threshold and remain OFF [22]. It is possible then, that cells in the OFF state were favoured during experimental evolution. This bistable behavior was first described in the lactose utilization system of *Escherichia coli* and has since become a central model for understanding phenotypic heterogeneity in bacterial populations.

In summary, our results demonstrate that our CRISPRi system is an effective tool for short-term inhibition of bacterial growth through repression of essential genes, while also revealing adaptive genetic changes that can rapidly compromise CRISPRi function under sustained selective pressure. These findings suggest that long-term silencing of essential genes may be improved by stabilizing inducer uptake, for example through the introduction of additional copies of the transporter genes placed under the control of constitutive promoters. Collectively, this work advances our understanding of the constraints and design principles governing CRISPRi-based manipulation of essential genes in non-model bacterial systems.

Methods

Bacterial strains and growth conditions

Bacterial strains and plasmids listed in **Supplementary Table 1** were grown in lysogeny broth (LB)-Lennox broth (Difco) at 37°C, with trimethoprim 100 µg/mL (Sigma-Aldrich) under continuous shaking at 230 rpm unless indicated otherwise. A stock solution of 20% L-rhamnose (Sigma-Aldrich) was prepared in filter-sterilized, deionized water and stored at room temperature. The sgRNA sequences and their target genes (locus tags) listed in **Supplementary Table 4** were obtained from Rahman *et al*. (2024). For genome sequencing glycerol stocks from short-term evolution experiments were thawed and 5 µL were inoculated in 5 mL of LB trimethoprim 100 µg/mL with/without 0.5% rhamnose for evolved and parental strains, respectively.

Characterization of Conditional Growth Phenotypes in CRISPRi Mutants

Overnight cultures, started from glycerol stocks, were grown in 5 mL LB with trimethoprim 100 µg/mL at 37°C and shaking at 230 rpm. To determine CGPs, cultures were back diluted to an OD_{600nm} 0.005 (~ 2.6 x 10^6 cells) and inoculated in a 96-well plate containing LB with trimethoprim 100 µg/mL with 0.5% rhamnose (dCas9-inducing) and without rhamnose (non-inducing). OD_{600nm} readings were taken at 1-hour intervals for 22 hours using a BioTek Synergy 2 microplate reader.

Short-term Experimental Evolution Assay

To assess prolonged gene silencing, three consecutive bacterial passages were performed under dCas9-inducing and non-inducing conditions. Three independent overnight cultures from glycerol stocks were back-diluted to an OD_{600nm} of 0.005 and inoculated in a 96-well plate containing LB trimethoprim 100 µg/mL and with/without 0.5% rhamnose. OD_{600nm} readings were taken at 1-hour intervals for 22 hours using a BioTek Synergy 2 microplate reader. At the end of the subculture, cell aliquots were collected as glycerol stocks in 20% glycerol and stored at -80°C. These stocks were used for subsequent overnight cultures, inoculating 5 µL in 5 mL of LB trimethoprim 100 µg/mL with/without 0.5% rhamnose to perform growth curves as previously described.

K-medoids or Partitioning Around Medoids (PAM) Clustering

Growth data from the short-term evolution assay were processed in R (version 4.3.2). using the R package Growthcurver [13]. The growth parameters listed in **Supplementary Table 3** were obtained, and the data were fitted to a standard logistic growth equation. To perform dimensionality reduction, the R packages "*factoextra*" [23] and "*cluster*" [24] were used to scale the data for standardization and to

reorganize the values into a table with growth parameters, biological replicates, and genes as columns. Distances between these values were calculated for further clustering. The optimal number of clusters was determined by the within sum of squares (WSS) and Silhouette methods (**Supplementary Fig. 21**). PAM or K-medoids algorithm was applied to specify the number of clusters.

Reverse transcription quantitative PCR (RT-qPCR) for parental and evolved strains

Glycerol stocks from the experimental evolution assay were grown under dCas9-inducing and non-inducing conditions. Parental strains were incubated without rhamnose, and evolved strains were incubated with rhamnose. Overnight cultures were diluted at an OD_{600nm} 0.01 and subcultured into fresh LB medium with trimethoprim 100 µg/mL, under both dCas9-inducing and non-inducing conditions. Cultures without rhamnose served as the control when calculating relative gene expression using the comparative CT method [25, 26]. Subcultures were incubated until mid-log phase (OD_{600nm} ~ 0.7) was reached, then harvested by centrifugation (5 min at 4000g). Total RNA was extracted using the PureLink™ RNA Mini Kit (Invitrogen) and purity (A260/280 ~ 2.0) was assessed by NanoDrop. Samples with concentrations ≥ 150 ng/µL were used for cDNA synthesis, performed with the SuperScript™ IV One-Step RT-PCR System (Invitrogen) using 1600 ng of RNA in a final reaction volume of 15 µL. Primers (**Supplementary Table 8**) were designed targeting the mid-region of the target gene, Tm between 58–62°C, GC content of 35–65%, and product sizes of 75–150 bp. Gene expression was normalized to the RNA polymerase sigma factor *sigE* (K562_RS21810). RT-qPCR was performed using PowerTrack SYBR Green Master Mix (Invitrogen) on a StepOnePlus Real-Time PCR System Applied Biosystems).[25, 26].

Whole Genome Sequencing, Assembly and SNP Identification

Genomic DNA from overnight cultures of the selected strains was extracted using the PureLink™ Microbiome DNA Purification Kit (Invitrogen). Concentrations were measured in a Qubit 2.0 Fluorometer. Samples were processed at Plasmidsaurus Inc. (Louisville, Kentucky, United States) for library preparation and Oxford Nanopore Sequencing (ONT). Twelve genomes (6 CRISPRi mutants under both conditions) were sequenced, each with a *minimum* coverage depth of 150x. De novo assembly was performed from raw data using Flye 2.9.4 [27]. The process was configured with a minimum overlap of 1000 bp and performing 10 iterative rounds to refine the assembly. All assemblies yielded five contigs, corresponding to three bacterial chromosomes, one mega plasmid, and a plasmid carrying the sgRNA and trimethoprim resistance cassette (pgRNA). Next, to enable pairwise comparisons, the FASTA output files were reordered manually in *Geneious* Software (Geneious Prime, version 8.1.9) to ensure the same starting positions. Pairwise genome comparisons were performed using Minimap2 version 2.28-r1209 [28] with a minimum overlap of 1000 bp. SyRI (Synteny and Rearrangement Identifier) SyRI (Synteny and Rearrangement Identifier) [29] was used to identify SNPs.

SDS-PAGE and Immunoblot to detect dCas9

Overnight cultures were inoculated from glycerol stocks and grown in 5 mL of LB trimethoprim 100 µg/mL. The cultures were diluted into 2 mL of fresh LB to an OD_{600nm} of 0.02 and grown until an OD_{600nm} of 0.7 was reached. Induction of dCas9 was performed by directly adding 0.5% rhamnose for 4 hours. Cultures were centrifuged, and cell pellets were resuspended in TNG buffer (100 mM Tris-HCl, 150 mM NaCl, 10% glycerol, pH 7.4). Cell lysis was performed by sonication with three cycles of 5 seconds, with a 5-second rest on ice between cycles. Total proteins were separated by 8% SDS-PAGE in duplicate. One SDS-PAGE gel was transferred to a polyvinylidene fluoride (PVDF) membrane using the iBlot system and blocked in 5% skim milk-TBST. Detection of dCas9 was performed using a primary mouse monoclonal antibody (ThermoFisher 10C11-A12) at room temperature for one hour, followed by three washes in TBST buffer (150 mM NaCl, 10 mM Tris-HCl, 0.5% Tween 20, pH 7.5). Then, a secondary goat anti-mouse antibody (ThermoFisher G-21060), linked to alkaline phosphatase, was added at a 1:20,000 dilution for 1 hour, followed by three washes in TBST buffer. Protein detection was done by chemiluminescence using a detection solution (5-bromo-4-chloro-3-indoyl phosphate [BCIP] in 1M Tris-HCl pH 9.5, 1M MgCl2, 2.5M NaCl). Results were visualized after 35 minutes.

Declarations

Additional Information (including a Competing Interests Statement)

The authors declare no competing interests.

Supplementary Information

Supplementary Figs. 1–21 and Supplementary Tables 1–4, 7–8 (word document)

Supplementary Table 5 (Excel file)

Supplementary Table 6 (Excel file)

Funding

This work was supported by the Natural Sciences and Engineering Research Council (NSERC) of Canada Discovery Grant (RGPIN04119-2022) and by the Canada Biomedical Research Fund and Biosciences Research Infrastructure Fund (Grant CBRF2-2023-00107).

Author Contribution

ZB – Performed all the experiments, data analysis and wrote the initial version of the manuscriptEAP – Cleaned data and performed data analysisASMZR – analyzed and interpreted results, and contributed to final editing of the manuscriptMP – Performed Python script and supervised bioinformatic analysisAMH – analyzed and interpreted results and contributed to the final editing of the manuscriptSY performed SNP analysis and prepared tablesYVB – provided financial support and contributed to the final editing of the manuscriptSTC – Conceived the idea, provided financial support, supervised the work, wrote and edited the final version of the manuscript

Data Availability

Assembled sequenced data from parental and evolved strains is available from the NCBI Sequencing Read Archive (SRA) under the BioProject ID PRJNA1255604. Single-nucleotide polymorphisms (SNPs) output files are provided in the Supplementary Materials.

References

1. Rancati, G., Moffat, J., Typas, A. & Pavelka, N. Emerging and evolving concepts in gene essentiality. *Nat. Rev. Genet.* **19**, 34–49 (2018).
2. Hogan, A. M. & Cardona, S. T. Gradients in gene essentiality reshape antibacterial research. *FEMS Microbiology Reviews* fuac005 (2022). 10.1093/femsre/fuac005
3. Qi, L. S. et al. Repurposing CRISPR as an RNA-guided platform for sequence-specific control of gene expression. *Cell* **152**, 1173–1183 (2013).
4. Cai, R., Lv, R., Shi, X., Yang, G. & Jin, J. CRISPR/dCas9 Tools: Epigenetic Mechanism and Application in Gene Transcriptional Regulation. *Int. J. Mol. Sci.* **24**, 14865 (2023).
5. Cui, L. et al. A CRISPRi screen in *E. coli* reveals sequence-specific toxicity of dCas9. *Nat. Commun.* **9**, 1912 (2018).
6. Hogan, A. M., Rahman, A. S. M. Z., Lightly, T. J. & Cardona, S. T. A broad-host-range CRISPRi toolkit for silencing gene expression in *Burkholderia*. *ACS Synth. Biol.* **8**, 2372–2384 (2019).
7. Liu, X. et al. High-throughput CRISPRi phenotyping identifies new essential genes in Streptococcus pneumoniae. *Mol. Syst. Biol.* **13**, 931 (2017).
8. Zhao, H. et al. Depletion of Undecaprenyl Pyrophosphate Phosphatases Disrupts Cell Envelope Biogenesis in *Bacillus subtilis*. *J. Bacteriol.* **198**, 2925–2935 (2016).
9. Rahman, A. S. M. Z. et al. Rationally designed pooled CRISPRi-seq uncovers an inhibitor of bacterial peptidyl-tRNA hydrolase. *Cell. Rep.* **43**, 114967 (2024).
10. Drevinek, P. & Mahenthiralingam, E. *Burkholderia cenocepacia* in cystic fibrosis: epidemiology and molecular mechanisms of virulence. *Clin. Microbiol. Infect.* **16**, 821–830 (2010).
11. Tavares, M., Kozak, M. & Balola, A. Sá-Correia, I. Burkholderia cepacia Complex Bacteria: a Feared Contamination Risk in Water-Based Pharmaceutical Products. *Clin. Microbiol. Rev.* **33**

10.1128/cmr.00139 – 19 (2020).

12. Gutiérrez Santana, J. C. & Coria Jiménez, V. R. *Burkholderia cepacia* complex in cystic fibrosis: critical gaps in diagnosis and therapy. *Ann Med* **56**, 2307503 .
13. Sprouffske, K. & Wagner, A. Growthcurver: an R package for obtaining interpretable metrics from microbial growth curves. *BMC Bioinform.* **17**, 172 (2016).
14. Khalil, A. S. & Collins, J. J. Synthetic biology: applications come of age. *Nat. Rev. Genet.* **11**, 367–379 (2010).
15. Gallagher, R. R., Patel, J. R., Interiano, A. L., Rovner, A. J. & Isaacs, F. J. Multilayered genetic safeguards limit growth of microorganisms to defined environments. *Nucleic Acids Res.* **43**, 1945–1954 (2015).
16. Fan, C. et al. Chromosome-free bacterial cells are safe and programmable platforms for synthetic biology. *PNAS* **117**, 6752–6761 (2020).
17. Egan, S. M. & Schleif, R. F. A Regulatory Cascade in the Induction of *rhaBAD*. *J. Mol. Biol.* **234**, 87–98 (1993).
18. Tate, C. G., Muiry, J. A. & Henderson, P. J. Mapping, cloning, expression, and sequencing of the rhaT gene, which encodes a novel L-rhamnose-H+ transport protein in Salmonella typhimurium and Escherichia coli. *J. Biol. Chem.* **267**, 6923–6932 (1992).
19. Cardona, S. T. & Valvano, M. A. An expression vector containing a rhamnose-inducible promoter provides tightly regulated gene expression in *Burkholderia cenocepacia*. *Plasmid* **54**, 219–228 (2005).
20. Hogan, A. M., Jeffers, K. R., Palacios, A. & Cardona, S. T. Improved dynamic range of a rhamnose-inducible promoter for gene expression in *Burkholderia* spp. *Appl. Environ. Microbiol.* **87**, e0064721 (2021).
21. Novick, A. & Weiner, M. Enzyme induction as an all-or-none phenomenon*. *Proceedings of the National Academy of Sciences* 43, 553–566 (1957).
22. Siegele, D. A. & Hu, J. C. Gene expression from plasmids containing the araBAD promoter at subsaturating inducer concentrations represents mixed populations. *Proc. Natl. Acad. Sci. U S A* 94, 8168–72 (1997).
23. Kassambara, A. & Mundt, F. Extract and Visualize the Results of Multivariate Data Analyses. (2020).
24. Maechler, M. et al. cluster: 'Finding Groups in Data': Cluster Analysis Extended Rousseeuw et al. (2025).
25. Livak, K. J. & Schmittgen, T. D. Analysis of relative gene expression data using real-time quantitative PCR and the 2(-Delta Delta C(T)) Method. *Methods* **25**, 402–408 (2001).
26. Schmittgen, T. D. & Livak, K. J. Analyzing real-time PCR data by the comparative CT method. *Nat. Protoc.* **3**, 1101–1108 (2008).
27. Kolmogorov, M., Yuan, J., Lin, Y. & Pevzner, P. A. Assembly of long, error-prone reads using repeat graphs. *Nat. Biotechnol.* **37**, 540–546 (2019).

28. Li, H. Minimap2: pairwise alignment for nucleotide sequences. *Bioinformatics* **34**, 3094–3100 (2018).
29. Goel, M., Sun, H., Jiao, W. B. & Schneeberger, K. SyRI: finding genomic rearrangements and local sequence differences from whole-genome assemblies. *Genome Biol.* **20**, 277 (2019).

Figures

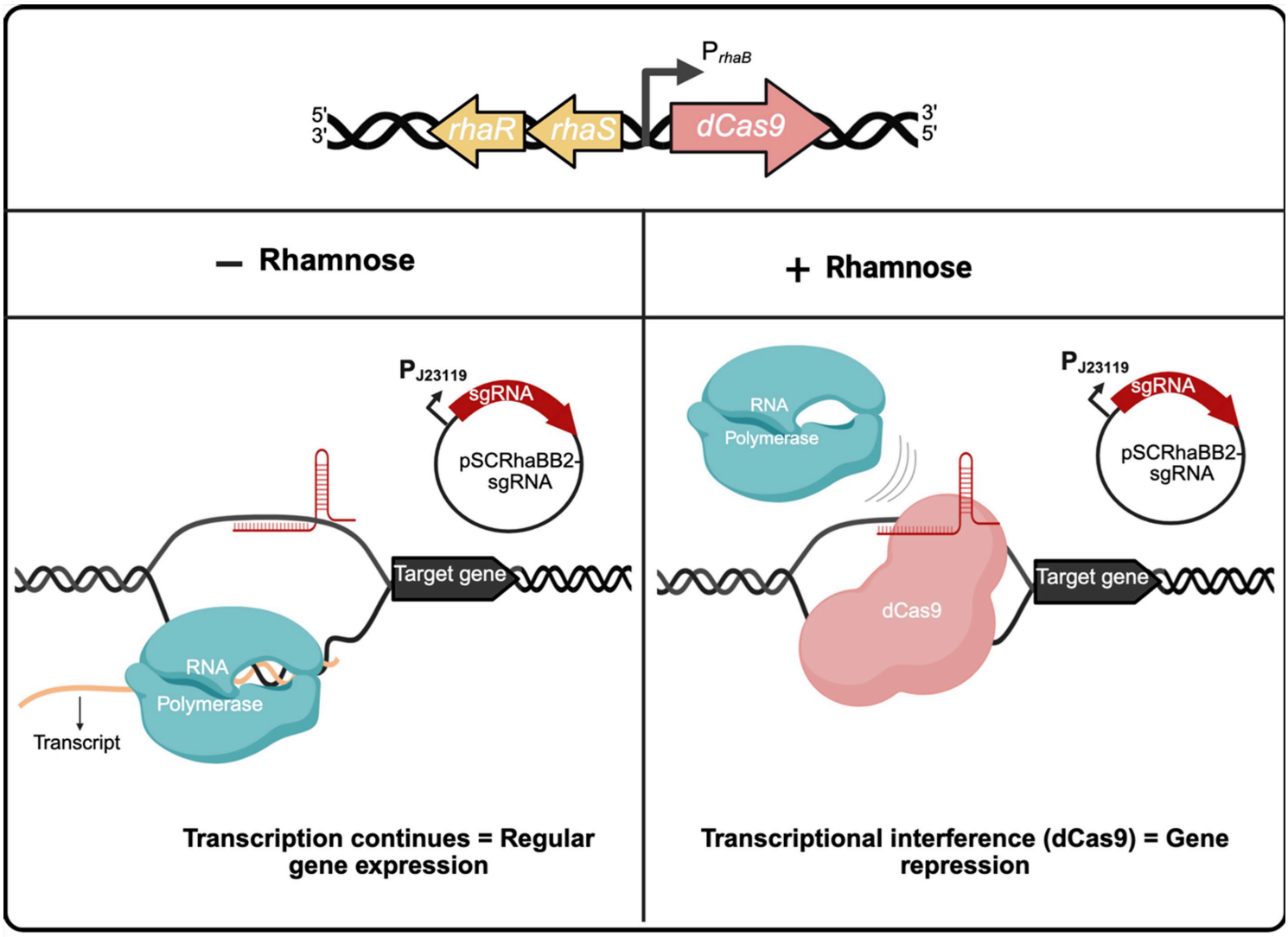


Figure 1

Rhamnose-inducible CRISPRi machinery in *B. cenocepacia* K56-2. The system consists of a chromosomally located *dCas9* gene regulated by P_{rhaB}, a rhamnose-inducible promoter. The sgRNAs are encoded in the plasmid pSCRhaB2-sgRNA and are expressed from the constitutive promoter P_{J23119}. Under dCas9-inducing conditions (+ rhamnose), rhamnose activates the promoter, leading to *dCas9* expression. dCas9 blocks transcription initiation or elongation by sterically interfering with the RNA polymerase. Adapted from [6].

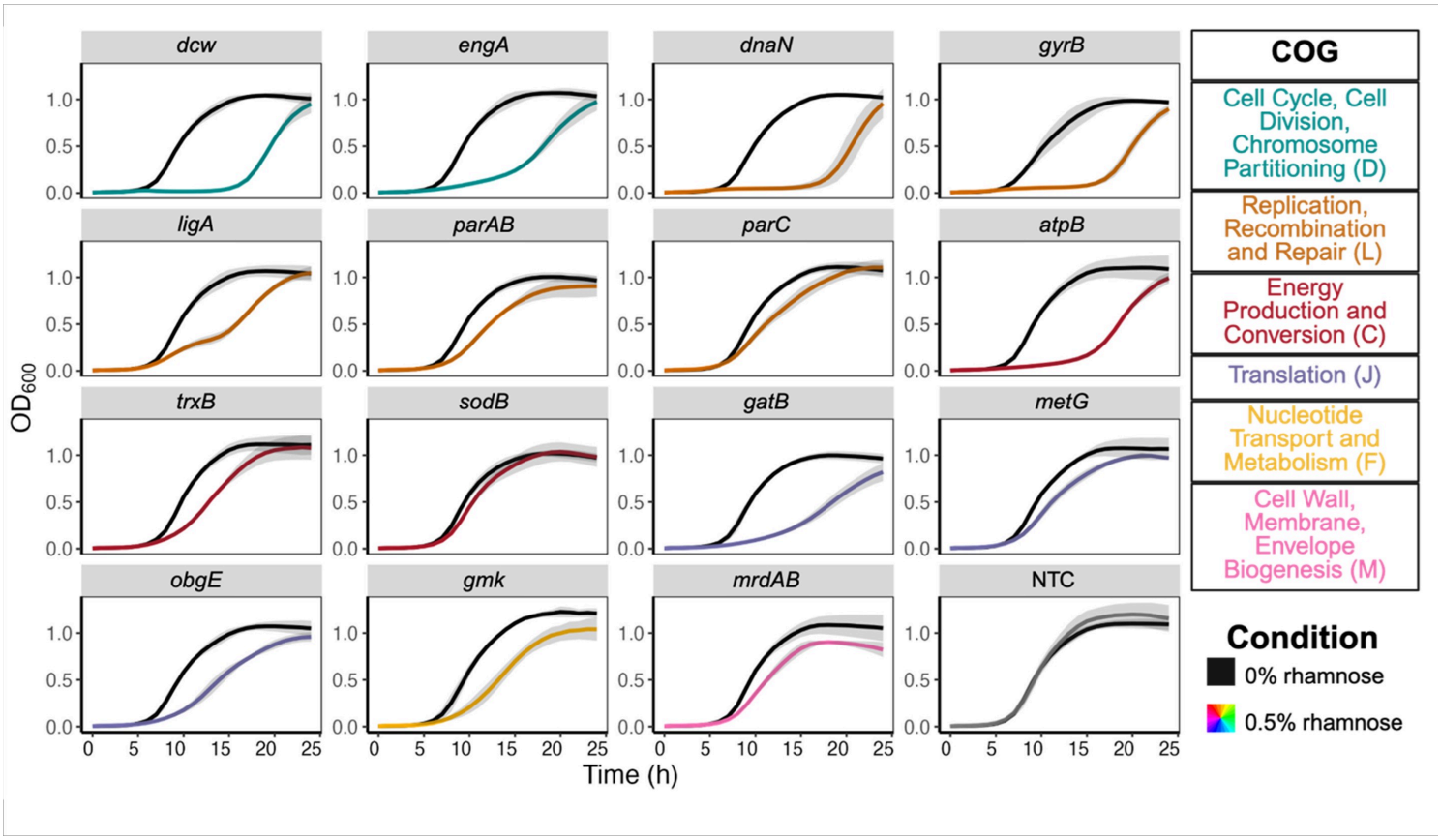


Figure 2

Conditional growth phenotypes (CGPs) of CRISPRi essential gene mutants. CRISPRi mutants were grown for 24 h in LB trimethoprim 100 µg/ml under dCas9-inducing conditions (0.5% rhamnose) or no rhamnose. Shaded areas indicate the standard deviation (arithmetic mean ± SD) from three independent biological replicates. NTC, nontargeting gRNA control.

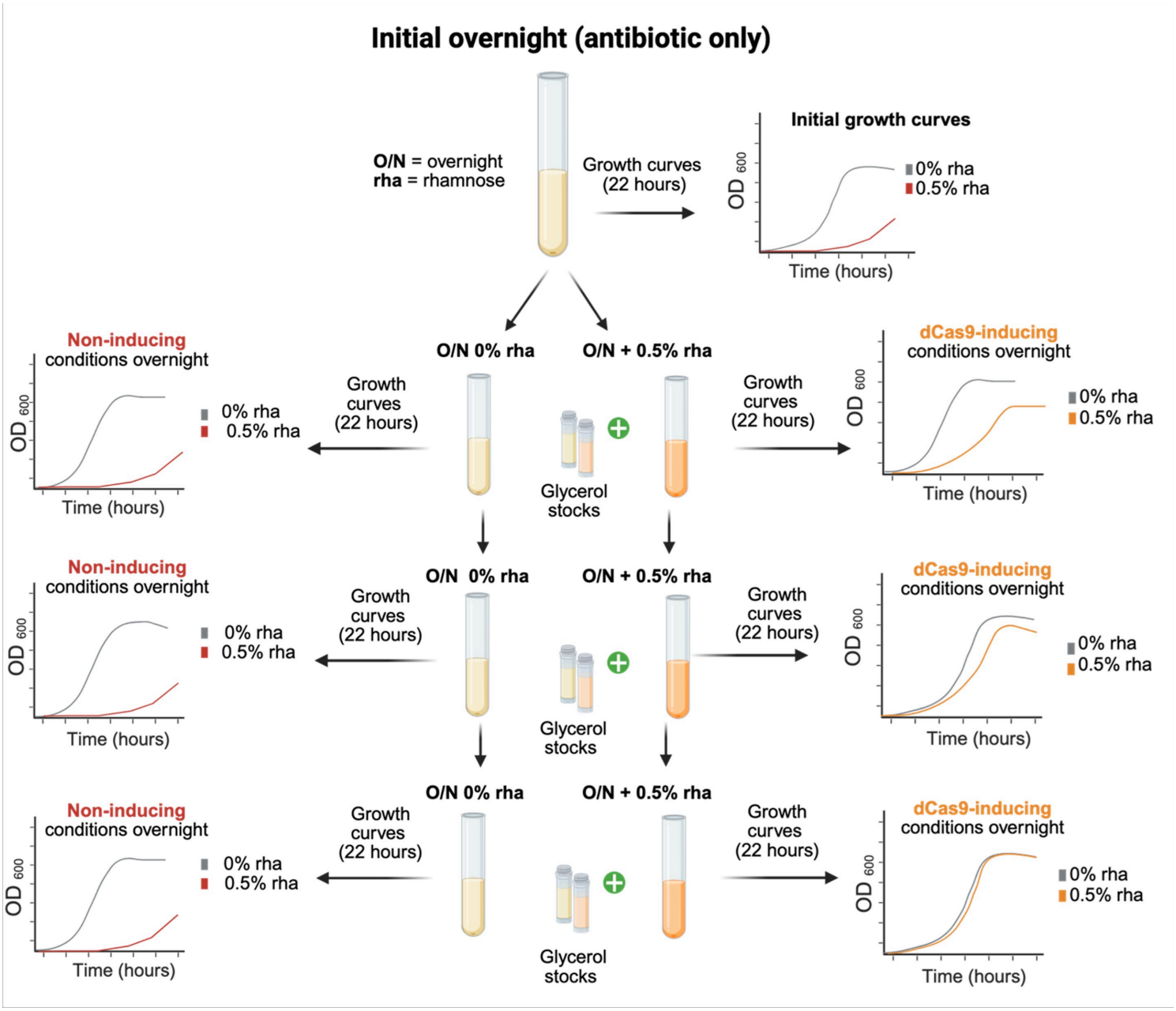


Figure 3

Workflow of the experimental evolution assay. A parental strain is cultured under non-inducing conditions, followed by growth-curve analysis performed under both dCas9-inducing and non-inducing conditions. Cultures are then subcultured into fresh medium under their respective conditions and incubated overnight (~16 h). After incubation, samples from each passage are preserved at –80 °C as glycerol stocks, thawed, and used as inocula for the subsequent passage. This process is repeated for a total of three consecutive passages. Expected outcomes at the time of the experimental design are illustrated: left panels depict the CGP after no rhamnose exposure during overnight growth, whereas right panels show the expected progressive CGP loss under continuous dCas9-inducing conditions across passages. All growth curves were initiated at an OD_{600} of 0.005, and three independent evolution replicates were performed for each CRISPRi mutant.

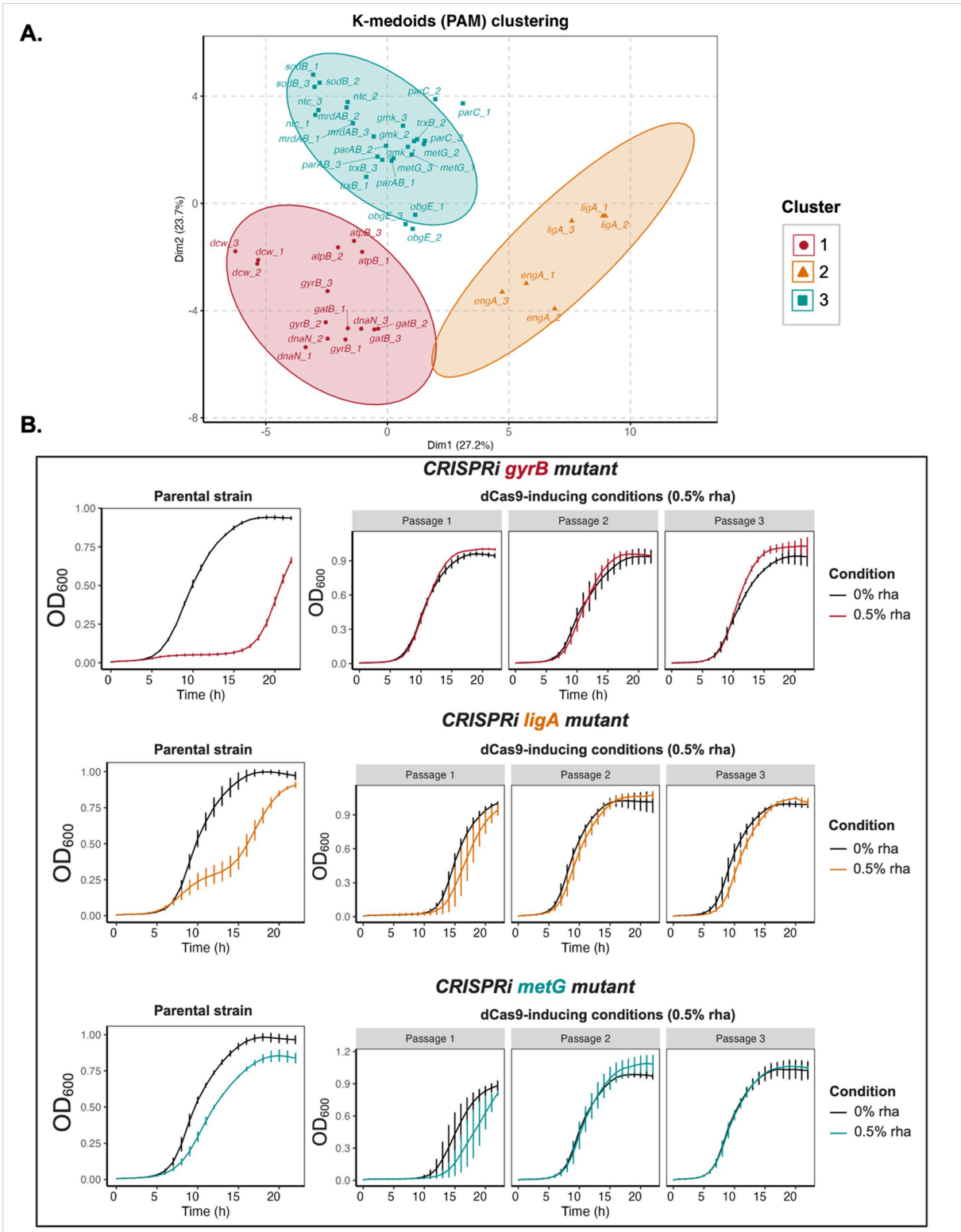


Figure 4

K-medoids clustering of CRISPRi mutants and identification of CGP loss during short-term evolution. (A) K-medoids analysis grouped the CRISPRi mutants into three clusters: Cluster 1 (*atpB, dnaN, gatB, gyrB, dcw*), Cluster 2 (*ligA, engA*), and Cluster 3 (*parAB, parC, metG, obgE, trxB, gmk, sodB, mrdAB*) plus the NTC control. Dimension 1 and Dimension 2 explain 27.2% and 23.7% of variance, respectively (50.9% total). Each point represents one of three biological replicates based on scaled growth parameters

across passages. (B) Representative growth curves under dCas9-inducing conditions showing CGP loss over serial passages. The *gyrB*, *ligA*, and *metG* mutants lose the CGP at different time points, while parental strains show severe, medium, or mild CGPs. The values represent three biological replicates ± SD; starting OD_{600} = 0.005.

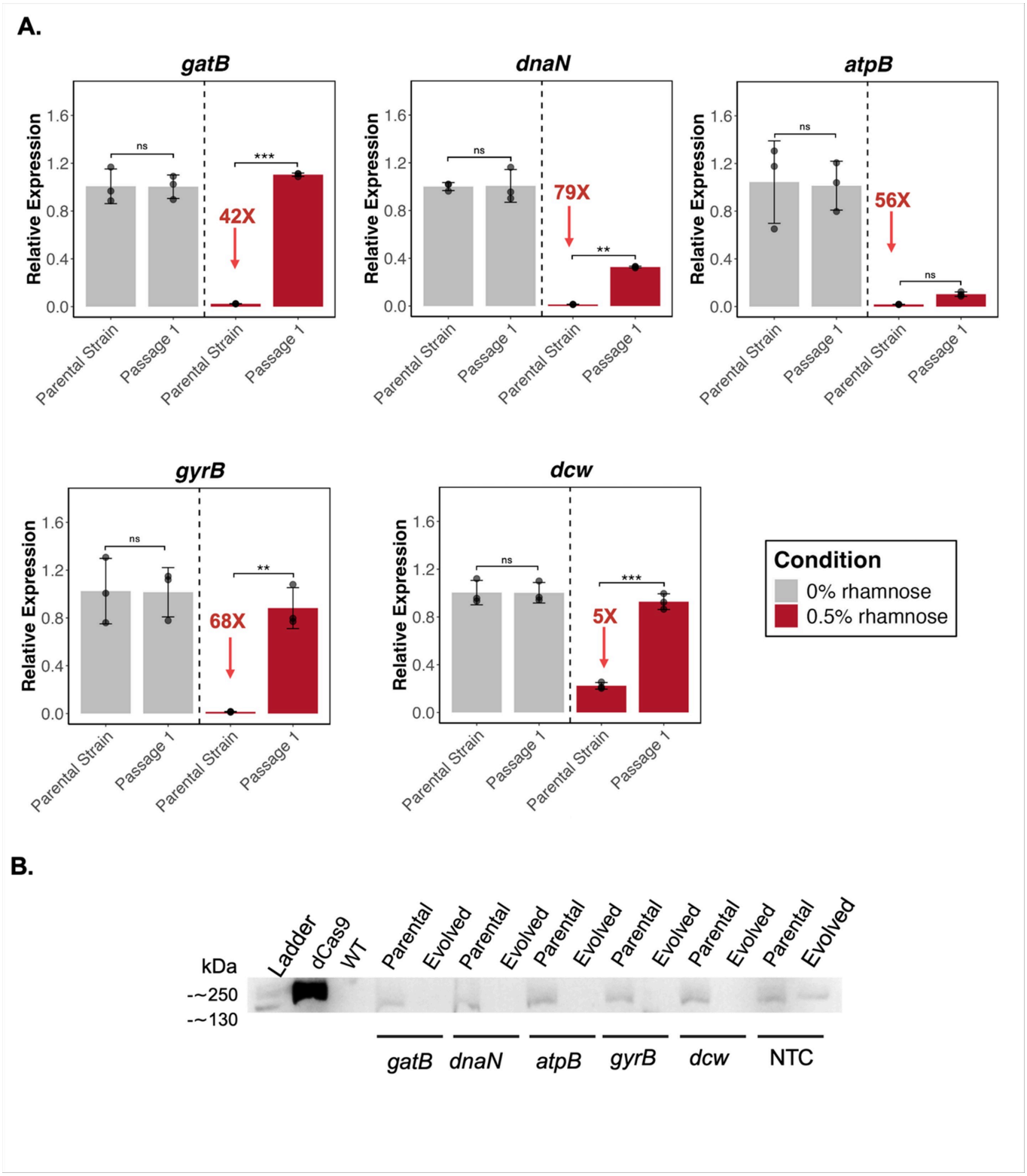


Figure 5

Target gene and dCas9 expression in parental and evolved CRISPRi mutants form Cluster 1. (A). Expression levels of the target genes in CRISPRi mutants were analyzed by RT-q-PCR in parental and evolved mutants under dCas9- non inducing (0% rhamnose) and inducing (0.5% rhamnose) conditions. Gene expression was normalized relative to *sigE* (sigma factor) and normalized to each parental strain under non-inducing conditions. Fold-change values were calculated using the 2^(ΔΔCt) method for data presentation. Statistical significance was determined using a two-way ANOVA with Tukey's post hoc test for multiple pairwise comparisons among all group means, performed on ΔΔCt values to assess the effects of condition and passage (***, $p < 0.001$; **, $p < 0.01$; *, $p < 0.05$). Black dots represent three independent biological replicates. (B). Immunoblot analysis of dCas9 expression in parental and evolved mutants, including purified dCas9, wild-type (WT), and non-targeting sgRNA control (NTC) strains. Cells were grown in LB supplemented with trimethoprim (100 µg/mL), induced with 0.5% rhamnose for 4 h, and analyzed by SDS–PAGE followed by immunoblotting using an anti-Cas9 monoclonal antibody and chemiluminescent detection. Loading controls and the full gel image are in Supplementary Figures 21 and 22.

Supplementary Files

This is a list of supplementary files associated with this preprint. Click to download.

- SupplementaryFigures121andSupplementaryTables14and78.docx
- SupplementaryTable5.xlsx
- SupplementaryTable6.xlsx